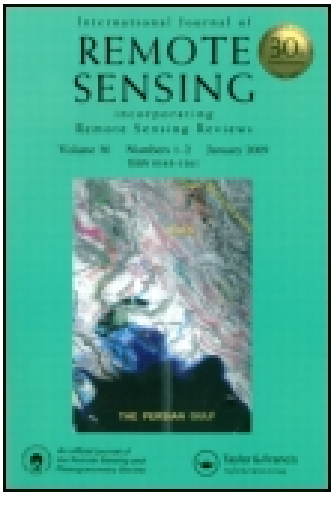

International Journal of Remote Sensing

Publication details, including instructions for authors and subscription information:
http://www.tandfonline.com/loi/tres20

Cloud climatology over the oceanic regions adjacent to the Indian Subcontinent: inter-comparison between passive and active sensors

Sagnik Dey[a], Nidhi Nishant[a], Kamalika Sengupta[a] & Sudipta Ghosh[a]
[a] Centre for Atmospheric Sciences, Indian Institute of Technology Delhi, Hauz Khas, New Delhi 110016, India
Published online: 17 Feb 2015.

To cite this article: Sagnik Dey, Nidhi Nishant, Kamalika Sengupta & Sudipta Ghosh (2015) Cloud climatology over the oceanic regions adjacent to the Indian Subcontinent: inter-comparison between passive and active sensors, International Journal of Remote Sensing, 36:3, 899-916

To link to this article: http://dx.doi.org/10.1080/01431161.2014.1001082

International Journal of Remote Sensing, 2015
Vol. 36, No. 3, 899–916, http://dx.doi.org/10.1080/01431161.2014.1001082

Taylor & Francis
Taylor & Francis Group

Cloud climatology over the oceanic regions adjacent to the Indian Subcontinent: inter-comparison between passive and active sensors

Sagnik Dey*, Nidhi Nishant†, Kamalika Sengupta‡, and Sudipta Ghosh

Centre for Atmospheric Sciences, Indian Institute of Technology Delhi, Hauz Khas, New Delhi 110016, India

(*Received 25 June 2014; accepted 27 November 2014*)

Understanding the cloud vertical structure and its variation in space and time is important to reduce the uncertainty in climate forcing. Here, we present the cloud climatology over the oceanic regions (Arabian Sea, Bay of Bengal, and South Indian Ocean) adjacent to the Indian subcontinent using data from the Multiangle Imaging Spectroradiometer (MISR), Moderate Resolution Imaging Spectroradiometer (MODIS), GCM-Oriented CALIPSO Cloud Product (GOCCP), and International Satellite Cloud Climatology Project (ISCCP). Fractional cloud cover (f_c) shows stronger seasonal variations over the Arabian Sea (mean annual f_c lies in the range 0.5–0.61) and Bay of Bengal (mean annual f_c lies in the range 0.69–0.75) relative to the South Indian Ocean (mean annual f_c lies in the range 0.64–0.71). Inter-comparison of statistics from passive (MISR, MODIS and ISCCP) and active (GOCCP) sensors reveals the challenges in interpreting satellite data for climate implications. While MISR detects more low clouds because of its stereo technique, MODIS and ISCCP detect more high clouds because of their radiometric techniques. Therefore, a combination of these two techniques in passive sensors may lead to more realistic understanding of the cloud vertical structure. GOCCP (active sensor) can detect multilayer cloud, but accuracy reduces if the high clouds are optically thick. A dominance of low and high clouds throughout the year is observed in these regions, where cumulus and cirrus dominate among low and high clouds, respectively.

1. Introduction

Aerosol–cloud–radiation interaction continues to be the largest source of uncertainty in quantifying anthropogenic climate change (IPCC 2007; Goren and Rosenfeld 2014; Altaratz et al. 2014). Large discrepancy among climate models in simulating clouds poses a challenge in resolving this critical problem (e.g. Zhang et al. 2005; Probst et al. 2012; Klein et al. 2013). Evaluation of model-simulated cloud distribution against satellite-based observation (e.g. Randall et al. 2003) at global and regional scales and inter-comparison of statistics from various sensors are required to address this issue (Stubenrauch et al. 2013). In addition to the cloud fraction, cloud vertical distribution (relative to aerosol vertical distribution) is equally important for improved estimates of radiative forcing.

Ground-based active remote sensing (e.g. lidar or radar) can be utilized to study the vertical distribution of clouds (Xi et al. 2010), but its limited spatial coverage, particularly over oceanic regions, restricts its applicability for regional scale study. Numerous passive

*Corresponding author. Email: sagnik@cas.iitd.ac.in
†Present address: Climate Change Research Center, University of New South Wales, Sydney, Australia.
‡Present address: School of Earth and Environment, University of Leeds, LS2 9JT, Leeds, United Kingdom.

sensors (e.g. sensors considered for the International Satellite Cloud Climatology Project (ISCCP), the Advanced Very High Resolution Radiometer (AVHRR), and the Moderate Resolution Imaging Spectroradiometer (MODIS)) have been using radiometric techniques for cloud retrieval, but they cannot retrieve cloud vertical structure at high vertical resolution. Retrieval of cloud vertical structure by passive remote sensing became possible with the advent of the stereo technique of the Multiangle Imaging Spectroradiometer (MISR) (Di Girolamo et al. 2010), which has been compared against the other passive (e.g. Naud et al. 2004; Marchand et al. 2010) and ground-based active sensors (Marchand, Ackerman, and Moroney 2007). Launches of Cloud-Aerosol Lidar and Pathfinder Satellite Observations (CALIPSO) and CloudSat in 2006 have provided a great opportunity to address this issue at various spatial and temporal scales (Anselmo et al. 2007; Verlinden, Thompson, and Stephens 2011; Nair et al. 2011; Meenu et al. 2010, 2011); however, the sampling noise due to the narrow swaths of the active space-borne sensors may be a concern in such inter-comparison. More observations over the years will resolve the sampling issue for the active sensors. Since cloud detection is a challenging task due to the influences of many remote-sensing artefacts such as misclassification of clear and cloudy pixels, shadow effect, and sun glint, as summarized in Loeb and Schuster (2008), there is a need to inter-compare multi-sensor data sets utilizing different retrieval techniques to understand the strengths and weaknesses of individual sensors. The importance of the issue led to an international effort initiated in 2005 under the umbrella of Global Energy and Water Cycle Experiment, which published its first coordinated inter-comparison of global cloud properties (Stubenrauch et al. 2013). More regional analysis (Jin, Hanesiak, and Barber 2007; Kühnlein et al. 2013), particularly in the regions affected by seasonal cycle of synoptic meteorology (e.g. Indian subcontinent), is warranted to fully understand the utility of satellite-based cloud products. In the present work, we utilize ten years of passive and five years of active remote-sensing data to examine the vertical distribution of clouds and its space-time variability over the oceanic regions adjacent to the Indian subcontinent.

The study area became a test bed for examining aerosol–cloud interaction, for which cloud vertical distribution is an important parameter (Chand et al. 2009), ever since the Indian Ocean Experiment (Ramanathan, Crutzen, Kiehl, et al. 2001). The Arabian Sea, Bay of Bengal and South Indian Ocean experience a reversal in wind direction from southwesterly during June to September to northeasterly during the winter months. The contrasting synoptic meteorology controls the precipitation pattern in the subcontinent and modulates aerosol characteristics by transporting polluted air from the land to the ocean during the winter season (Ramanathan, Crutzen, Kiehl, et al. 2001). Also, cloud detection is easier over ocean relative to land due to homogeneous surface reflectance (excluding the glint-affected areas), and hence, the inter-comparison will help better understanding of the strength and weakness of the retrieval techniques in detecting cloud vertical structure.

Variability of clouds over global oceans has been examined from 55 years of surface observations (Eastman, Warren, and Hahn 2011). However, very few studies exist in the Indian Continental Tropical Convergence Zone. Combined analysis of ISCCP and Earth Radiation Budget Experiment flux data for the period 1985–1988 was carried out by Rajeevan and Srinivasan (1999) to understand the variability of cloud radiative forcing (CRF) in this region. Using the same data sets, Patil and Yadav (2005) have estimated much larger shortwave (SW) cooling than longwave (LW) warming for the monsoon clouds over the Indian region. The resulting net cooling at the top-of-the-atmosphere (TOA) was found to be larger over the Bay of Bengal relative to the Arabian Sea in the monsoon season due to a larger fractional

cloud cover (f_c) facilitated by the upper tropospheric easterly jet (Sathiyamoorthy, Pal, and Joshi 2011). From a satellite point of view, f_c is defined as the fraction of cloudy pixels in the total number of pixels within a given domain. Wonsick, Pinker, and Govaerts (2009) examined the diurnal variation of f_c over the Indian region using Meteosat observations and observed that the daytime diurnal cycles are flat, U-shaped, and ascending towards an afternoon peak during the pre-monsoon, monsoon, and post-monsoon seasons, respectively. Meenu et al. (2010, 2011) examined the variability of high clouds over the subcontinent using CALIPSO data and reported occurrence of the deepest clouds (12 K lower than other deep convective regions) over the northern Bay of Bengal during June–August. Nair et al. (2011) found a 'pool of inhibited cloudiness' over the Bay of Bengal during the monsoon months by combining CloudSat and AVHRR data. Most of these studies used satellite data of limited period of time. For example, Bony, Collins, and Fillmore (2000) examined the variability of low clouds in the winter season during 1986–1989 and observed that the Arabian Sea and Bay of Bengal are dominated by cumulus clouds, while the South Indian Ocean is dominated by stratocumulus clouds. Moreover, they are confined to mostly passive remote sensing. Therefore, there is a need to understand the space–time variability of clouds for a longer period of time, and more particularly, their vertical distributions in the Indian monsoon region in the recent years. Changes in precipitation pattern over the Indian monsoon region in the recent years (Goswami et al. 2006; Dash et al. 2009) further emphasize the importance to understand the variability of cloud vertical structure.

Here, we present a monthly climatology of f_c over the Arabian sea, Bay of Bengal, and South Indian Ocean derived from MISR and MODIS for the period March 2000–February 2010, GCM-Oriented CALIPSO Cloud Product (GOCCP) for the period June 2006–December 2010, and ISCCP for the period January 2000–December 2007. Further, ISCCP data for the period 2000–2007 have been used to examine the relative abundance of individual cloud types. This will help in interpreting the observed variability in cloud distribution statistics from passive and active sensors. The applicability of such climatological statistics for climate studies is discussed in view of the strengths and weaknesses of the retrieval techniques.

2. Analysis

Since our objective is to understand the variability of cloud vertical distribution over the oceans surrounding the Indian subcontinent, we chose the domain as follows: the Arabian Sea bounded by 20° N to the equator and 58–73° E longitude, the Bay of Bengal bounded by 20° N to the equator and 86–94° E, and the South Indian Ocean bounded by the equator to 20° S and 58–94° E longitude (Figure 1). We analysed MISR cloud fraction by altitude (CFbA) and MODIS cloud products for ten years (March 2000–February 2010), GOCCP-f_c for five years (June 2006–December 2010) and ISCCP data for eight years (January 2000–December 2007). Mean monthly statistics have been generated for f_c, its vertical distribution, and relative abundance of various individual cloud types. f_c may vary simply because of different cloud detection techniques (Stubenrauch et al. 2013) and/or different pixel resolutions of various sensors (Zhao and Di Girolamo 2006). While comparing climatology of f_c and cloud vertical distribution, only daytime retrievals are considered because MISR can detect clouds only in daytime. Brief descriptions of the satellite and other data are provided below.

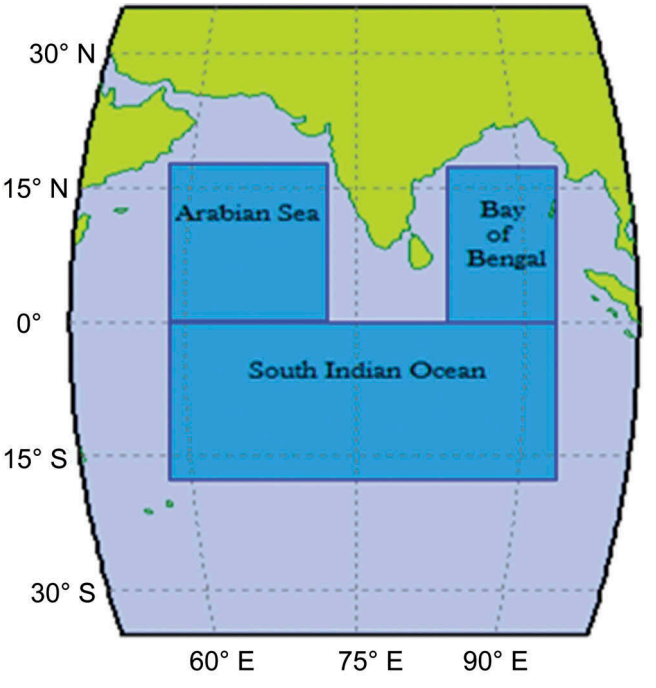

Figure 1. Locations of the study area: the Arabian Sea, Bay of Bengal, and South Indian Ocean.

2.1. MISR Data

MISR, on board EOS-Terra, crosses the equator at ~10:30/22:30 local time. It has nine cameras at 0°, ±26.1°, ±45.6°, ±60°, and ±70.5°. Choosing a multi-angle view over a single nadir viewing sensor ensures almost an order of magnitude improvement in the accuracy of individual scene albedo and better probing into the cloud vertical height. Cloud top height is determined using the three near nadir cameras 0° and ±26° using the stereo technique at 1.1 km × 1.1 km resolution at sufficient spatial contrast between cloud and underlying surface (Marchand et al. 2010). This technique does not rely on atmospheric thermal structure and is less sensitive to radiometric calibration error (Di Girolamo et al. 2010). The relative frequency of cloud tops at each 0.5 km vertical resolution is processed as level 3 daily (and subsequently as monthly by averaging all daily values) CFbA products gridded globally at 0.5° × 0.5° spatial resolution between the surface and 20 km altitude (Di Girolamo et al. 2010). Detailed discussion about the quality of MISR cloud top height retrieval is available in the literature (e.g. Marchand, Ackerman, and Moroney 2007, 2010; Naud et al. 2004). In brief, the major source of error in cloud top height detection stems from 'wind correction' with each 1 m s^{-1} error in the along-track wind leading to an error of ~100 m in the cloud top height (Marchand et al. 2010). It must be mentioned here that this technique relies on the optical depth threshold and thus fails to identify thin (cloud optical depth (COD) in the range 0.1–0.3) and sub-visual cirrus (COD < 0.1) (Prasad and Davies 2012). However, this also allows detection of low-level clouds beneath thin cirrus. To compare with columnar f_c from MODIS and ISCCP, MISR f_c values of each altitude bin are summed to derive the columnar f_c.

2.2. MODIS Data

MODIS is flying on board EOS-Terra along with MISR and also on Aqua (which crosses the equator at ~13:30/1:30 local time). It uses both SW and thermal infrared bands only at the nadir view to detect clouds. Multispectral retrieval mitigates the concern of inappropriate cloud classification while encountering snow and ice conditions. Additionally a CO_2 slicing technique (Wylie, Menzel, and Strabala 1994) is employed to distinguish transmissive clouds from opaque clouds and thus helps to report thin cirrus clouds, which are often missed by the other sensors (e.g. Ackerman et al. 2002). Cloud masking is done at 1 km × 1 km resolution and f_c is calculated as the ratio of cloudy pixels to the total number of pixels within a domain of 10 km × 10 km (Level 2 data) (Platnick et al. 2003). The level 2 f_c is further averaged over 1° × 1° spatial resolution to produce a daily and monthly level 3 f_c product. In the present study, daytime Terra-MODIS derived f_c data are analysed for comparison with MISR-derived f_c.

2.3. ISCCP Data

Cloud-type information has been derived from the ISCCP D2 data set (Rossow and Schiffer 1999). ISCCP uses up to five geostationary and two polar orbiting satellites to calculate f_c at three hour intervals. The clouds detected are further classified into nine types according to cloud top pressure (CTP) and COD. Clouds are first categorized as 'low clouds' (when CTP is below 680 hPa altitude), 'mid-level clouds' (when CTP lies between 440 hPa and 680 hPa altitude), and 'high clouds' (when CTP exceeds 440 hPa altitude). Each of these three cloud types are further subdivided into three categories based on COD. Low clouds with COD < 3.6, 3.6 < COD < 23, and COD > 23 are classified as cumulus, stratocumulus, and stratus, respectively. The corresponding classes for mid-level clouds are altocumulus, altostratus, and nimbostratus; while the classes are cirrus, cirrostratus, and deep convective, respectively, for high clouds. The D2 data set is an improvement over the previous data sets because of the reduction of the bias in retrieved cloud top temperature and pressure. This has been achieved by including effects of infrared scattering, improved low-level cloud sensitivities during the sunrise and sunset, and by changing the visible radiance threshold test to a visible reflectance threshold test (Rossow and Schiffer 1999). However, very thin clouds (COD < 0.1 over ocean) may be missed by ISCCP. In the present study, we analysed ISCCP data at 6 UTC (11:30 am local time), which is in between Terra (10:30 am local time) and CALIPSO (~1:30 pm local time) overpass times to facilitate inter-comparison.

2.4. GOCCP data

Cloud vertical distributions are also available from the GOCCP data sets. The detailed algorithm is discussed by Chepfer et al. (2010). First, clouds are detected based on the scattering ratio (SR) thresholds in the measured vertical profiles at 333 m resolution below 8 km and at 1 km resolution above 8 km. For example, cloudy (SR > 5), clear (0.01 < SR < 1.2), fully attenuated (SR < 0.01), and unclassified (1.2 < SR < 5) layers are identified in the profiles. Then it is determined whether the profile contains at least one 'low cloud' (CTP below 680 hPa altitude), 'mid-level cloud' (440 < CTP <680 hPa), and 'high cloud' (CTP above 440 hPa altitude). Monthly f_c is computed at 40 vertical levels between surface to 19.2 km at 480 m interval, for each 1° × 1° grid box by considering the number of cloudy profiles in total SR profiles in one month. Note that this definition is

different from the definition of f_c (i.e. fraction of cloudy pixels to total number of pixels within a scene) in the passive remote sensing. The fully attenuated profiles are not considered in generating cloud vertical distributions in GOCCP data sets. This is done to increase the signal-to-noise ratio and minimize false cloud detection (Chepfer et al. 2010). This data set was produced with the view of making satellite observations of the cloud field more coherent with the ensemble GCM and lidar simulator-simulated cloud fields (with respect to horizontal and vertical resolution, cloud detection, and cloud diagnostics) so that a comparison between the two could bring out the shortcomings of the model performance rather than the differences in the methods applied by the model and simulator outputs and the observations. Thus like most GCMs, this data set has the cloud vertical distribution at 40 altitude bins making it suitable for comparison with MISR. Since CALIOP is an active remote sensor, both day and night-time cloud vertical distributions are available. For the comparison with other data sets, only daytime GOCCP data version 2.69 is analysed.

3. Results

3.1. *Variability of f_c*

The temporal variability of f_c from various sensors is shown in Figure 2, while the mean (±1 standard deviation, σ) monthly statistics are summarized in Table 1. The climatology was derived from the multi-sensor observations within a 3-hour window (10:30 am–1:30 pm) to minimize the influence of diurnal variability on f_c. The seasonal variability of f_c is strong over the Arabian Sea and Bay of Bengal, with highest values of f_c (0.7–0.9) in the monsoon

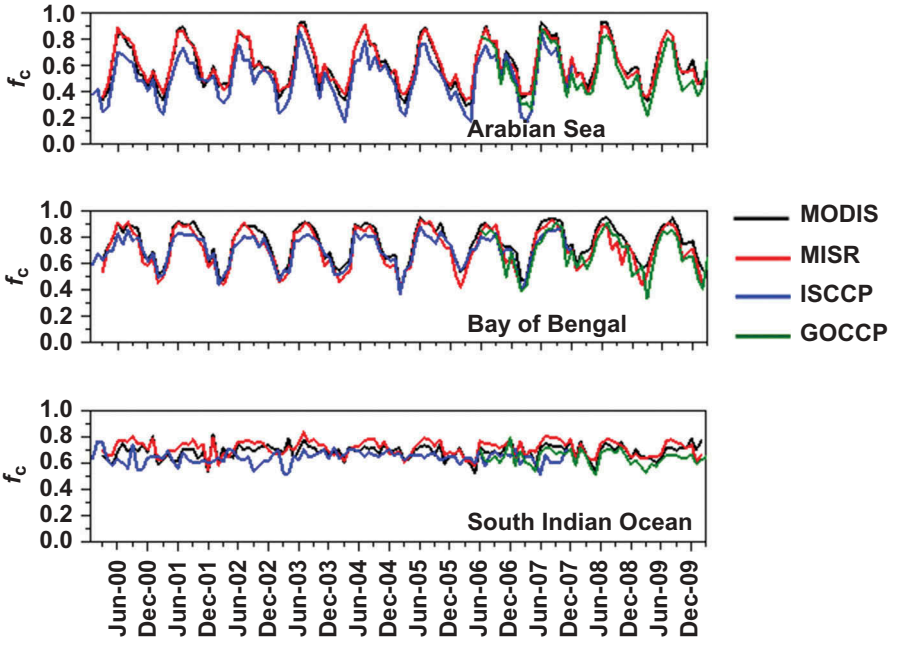

Figure 2. Temporal variability of f_c from MISR and MODIS (during March 2000–February 2010), ISCCP (during January 2000–December 2007), and GOCCP (during June 2006–February 2010) over the Arabian Sea, Bay of Bengal, and South Indian Ocean.

Table 1. Mean ($\pm 1\sigma$) monthly statistics of f_c from various sensors over the Arabian Sea (1st row), Bay of Bengal (2nd row), and South Indian Ocean (3rd row).

	MODIS-f_c (day)	MISR-f_c (day)	ISCCP-f_c (day)	GOCCP-f_c (day)	GOCCP-f_c (night)	MODIS-f_c (night)
Time period	March 2000–February 2010	March 2000–February 2010	January 2000–December 2007	June 2006–February 2010	June 2006–February 2010	March 2000–February 2010
January	0.53 ± 0.05	0.53 ± 0.04	0.44 ± 0.05	0.43 ± 0.07	0.46 ± 0.04	0.51 ± 0.05
	0.64 ± 0.04	0.57 ± 0.05	0.61 ± 0.06	0.53 ± 0.03	0.48 ± 0.05	0.55 ± 0.02
	0.71 ± 0.06	0.68 ± 0.06	0.66 ± 0.04	0.59 ± 0.02	0.62 ± 0.04	0.73 ± 0.02
February	0.40 ± 0.06	0.43 ± 0.06	0.44 ± 0.07	0.38 ± 0.08	0.35 ± 0.11	0.39 ± 0.10
	0.52 ± 0.08	0.45 ± 0.05	0.49 ± 0.10	0.51 ± 0.13	0.45 ± 0.11	0.50 ± 0.12
	0.70 ± 0.07	0.67 ± 0.06	0.65 ± 0.06	0.65 ± 0.06	0.69 ± 0.08	0.78 ± 0.05
March	0.36 ± 0.06	0.38 ± 0.03	0.29 ± 0.05	0.31 ± 0.06	0.28 ± 0.04	0.32 ± 0.07
	0.56 ± 0.07	0.51 ± 0.05	0.54 ± 0.05	0.45 ± 0.10	0.46 ± 0.12	0.54 ± 0.10
	0.65 ± 0.04	0.65 ± 0.03	0.64 ± 0.06	0.61 ± 0.06	0.63 ± 0.06	0.73 ± 0.03
April	0.45 ± 0.06	0.44 ± 0.03	0.23 ± 0.09	0.35 ± 0.06	0.33 ± 0.05	0.39 ± 0.05
	0.66 ± 0.06	0.61 ± 0.07	0.62 ± 0.06	0.57 ± 0.07	0.56 ± 0.06	0.68 ± 0.05
	0.66 ± 0.06	0.67 ± 0.03	0.65 ± 0.06	0.57 ± 0.04	0.59 ± 0.04	0.70 ± 0.04
May	0.66 ± 0.04	0.65 ± 0.05	0.55 ± 0.05	0.58 ± 0.07	0.57 ± 0.08	0.66 ± 0.06
	0.84 ± 0.04	0.81 ± 0.05	0.75 ± 0.05	0.77 ± 0.03	0/76 ± 0.04	0.86 ± 0.04
	0.61 ± 0.06	0.67 ± 0.04	0.64 ± 0.04	0.57 ± 0.07	0/59 ± 0.03	0.65 ± 0.06
June	0.86 ± 0.05	0.85 ± 0.04	0.74 ± 0.08	0.80 ± 0.08	0.81 ± 0.08	0.84 ± 0.08
	0.90 ± 0.03	0.88 ± 0.03	0.81 ± 0.04	0.84 ± 0.05	0.88 ± 0.02	0.94 ± 0.02
	0.69 ± 0.04	0.74 ± 0.03	0.63 ± 0.06	0.67 ± 0.03	0.69 ± 0.06	0.74 ± 0.03
July	0.89 ± 0.03	0.87 ± 0.03	0.73 ± 0.05	0.83 ± 0.03	0.81 ± 0.05	0.87 ± 0.03
	0.90 ± 0.03	0.89 ± 0.02	0.81 ± 0.03	0.86 ± 0.04	0.91 ± 0.03	0.96 ± 0.02
	0.73 ± 0.03	0.78 ± 0.03	0.64 ± 0.04	0.67 ± 0.04	0.71 ± 0.03	0.76 ± 0.03
August	0.79 ± 0.03	0.80 ± 0.02	0.64 ± 0.03	0.79 ± 0.04	0.77 ± 0.03	0.80 ± 0.03
	0.90 ± 0.03	0.88 ± 0.07	0.81 ± 0.07	0.85 ± 0.02	0.90 ± 0.06	0.95 ± 0.03
	0.71 ± 0.02	0.77 ± 0.02	0.64 ± 0.04	0.69 ± 0.05	0.73 ± 0.03	0.77 ± 0.03
September	0.70 ± 0.08	0.71 ± 0.08	0.61 ± 0.09	0.67 ± 0.10	0.67 ± 0.10	0.71 ± 0.09
	0.88 ± 0.03	0.83 ± 0.04	0.80 ± 0.03	0.84 ± 0.05	0.89 ± 0.03	0.93 ± 0.04
	0.70 ± 0.02	0.77 ± 0.03	0.65 ± 0.06	0.67 ± 0.02	0.72 ± 0.04	0.77 ± 0.02

(*Continued*)

Table 1. (*Continued*).

	MODIS-f_c (day)	MISR-f_c (day)	ISCCP-f_c (day)	GOCCP-f_c (day)	GOCCP-f_c (night)	MODIS-f_c (night)
Time period	March 2000–February 2010	March 2000–February 2010	January 2000–December 2007	June 2006–February 2010	June 2006–February 2010	March 2000–February 2010
October	0.56 ± 0.06	0.58 ± 0.05	0.50 ± 0.07	0.49 ± 0.06	0.48 ± 0.08	0.55 ± 0.06
	0.82 ± 0.07	0.73 ± 0.08	0.76 ± 0.07	0.74 ± 0.10	0.75 ± 0.09	0.84 ± 0.07
	0.70 ± 0.04	0.74 ± 0.02	0.62 ± 0.04	0.66 ± 0.05	0.72 ± 0.05	0.76 ± 0.05
November	0.54 ± 0.09	0.54 ± 0.07	0.54 ± 0.10	0.47 ± 0.10	0.43 ± 0.10	0.55 ± 0.06
	0.73 ± 0.07	0.67 ± 0.07	0.73 ± 0.05	0.63 ± 0.10	0.64 ± 0.09	0.75 ± 0.03
	0.70 ± 0.04	0.73 ± 0.03	0.65 ± 0.05	0.65 ± 0.02	0.70 ± 0.02	0.76 ± 0.02
December	0.56 ± 0.09	0.53 ± 0.07	0.49 ± 0.09	0.48 ± 0.04	0.50 ± 0.07	0.59 ± 0.03
	0.70 ± 0.06	0.65 ± 0.06	0.67 ± 0.05	0.65 ± 0.09	0.69 ± 0.06	0.71 ± 0.06
	0.69 ± 0.08	0.69 ± 0.07	0.65 ± 0.04	0.67 ± 0.09	0.71 ± 0.07	0.78 ± 0.07

(June–September) season as expected, and lowest values (0.4–0.5) in the winter season (December–February) as revealed by the passive (MODIS, MISR, and ISCCP) and active (GOCCP) sensors (Figure 2). GOCCP shows a slight low bias in f_c in the monsoon season, which may stem from the way f_c is defined as a direct consequence of the lidar limitation. The monsoon season is characterized by the development of optically thick convective clouds. If the lidar signal becomes attenuated due to penetration through optically thick clouds, the number of times low-level clouds are detected within a grid will be reduced and thus f_c will also be reduced. The passive sensors detect the cloud tops and calculate f_c by counting the number of cloudy pixels within the grid. Seasonal variability of f_c is much lower over the South Indian Ocean compared to the Arabian Sea and Bay of Bengal as shown by the passive and active sensors (Table 1). This may be attributed to less seasonal variability of synoptic scale meteorology and low aerosol concentration, thereby less influence on cloud formation, over the South Indian Ocean. The mean ($\pm 1\sigma$) annual f_c values over the Arabian Sea are 0.61 ± 0.18, 0.61 ± 0.17, 0.5 ± 0.17, and 0.55 ± 0.19 as estimated by MODIS, MISR, ISCCP, and GOCCP, respectively. The corresponding values for the Bay of Bengal are 0.75 ± 0.14, 0.71 ± 0.16, 0.70 ± 0.12, and 0.69 ± 0.16, and for the South Indian Ocean are 0.69 ± 0.06, 0.71 ± 0.06, 0.64 ± 0.05, and 0.64 ± 0.06, respectively. We note here that some difference in the statistics (Table 1) between the active and passive sensors may arise from different time periods of observations (Wu et al. 2009). More regional scale analysis may resolve this issue, but this further emphasizes the importance of understanding height-stratified cloudiness in interpreting the cloud variability (Stubenrauch et al. 2013).

Figure 3 shows the inter-comparison between f_c from MISR ($f_{c,\mathrm{MISR}}$) and MODIS ($f_{c,\mathrm{MODIS}}$) over the three oceanic regions. $f_{c,\mathrm{MISR}}$ retrieved using the stereo technique and $f_{c,\mathrm{MODIS}}$ retrieved using radiometric technique match very well throughout the entire ten-year period with a high degree of correlations (correlation coefficients (R) are 0.98, 0.96, and 0.77, respectively, for the Arabian Sea, Bay of Bengal, and South Indian Ocean, which are significant at 99% confidence interval). The maximum difference is ~3% over the Arabian Sea and ~10% over the Bay of Bengal during the winter season and 7–9%

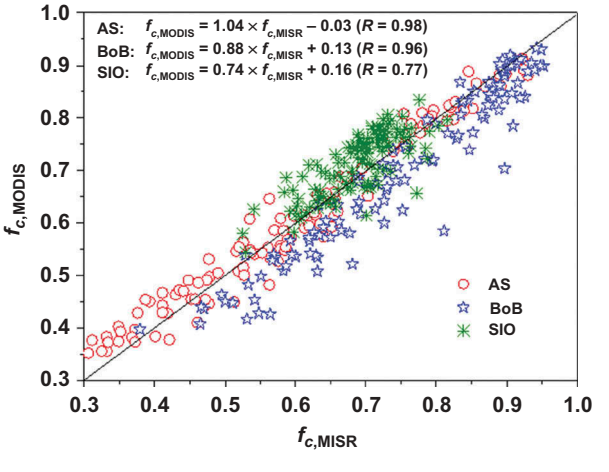

Figure 3. Correlations between MISR and MODIS-derived f_c over the Arabian Sea (AS), Bay of Bengal (BoB), and South Indian Ocean (SIO) for the same period. The correlation coefficients and equations of the best-fit lines are also given. The solid line represents the 1:1 line.

during the monsoon season over the South Indian Ocean (Table 1). Several factors may lead to this observed discrepancy. Note that f_c is dominated by low clouds (mostly cumulus and stratocumulus) during these periods in the respective regions; hence the 'resolution effect' may contribute to the discrepancy (Zhao and Di Girolamo 2006). The view angle geometry of MODIS may be another factor (Maddux, Ackerman, and Platnick 2010). Different cloud detection techniques and sampling frequency in generating the climatology may also contribute to this discrepancy. For example, a large amount of cirrus clouds are detected by GOCCP and ISCCP over the South Indian Ocean during the monsoon season, which may be missed by MISR (Prasad and Davies 2012) and detected by MODIS due to their respective cloud detection techniques.

Although the sensors show some discrepancy in the absolute values of f_c, the seasonality shows appreciable match between all sensors. The seasonality in f_c over these regions is influenced by synoptic meteorology and aerosols. Aerosol optical depth, AOD at 558 nm wavelength is obtained from MISR. Quality and applicability of MISR AOD in this region were discussed in earlier studies (Dey and Di Girolamo 2010). Large AOD (>0.25) over the Arabian Sea and Bay of Bengal (compared to typical background maritime AOD of <0.15, Smirnov et al. 2009) may facilitate cloud formation within a favourable SST range, but f_c becomes saturated at high SST (Gadgil, Joseph, and Joshi 1984; Nair et al. 2011). During the winter season, a large fraction of AOD is absorbing components transported from the Indian landmass (Kedia et al. 2012), which co-exist with cumulus clouds in the same altitude range (Ramanathan et al. 2007). Cumulus dominates among the low-level clouds in this region (Bony, Collins, and Fillmore 2000 and also observed in ISCCP climatology as shown in Figure 5), thus the chance of aerosol–cloud interaction is high (Dey et al. 2011) in this season. Very low aerosol concentration throughout the year over the South Indian Ocean implies a stronger connection of clouds with meteorology than with aerosols. Eastman, Warren, and Hahn (2011) observed that f_c does not always show direct positive correlation with SST because of the competing influences of other meteorological parameters and aerosols. For example, formation of low clouds (mostly cumulus; Bony, Collins, and Fillmore 2000) may continue over the Arabian Sea and Bay of Bengal even during the development of high clouds, probably due to the presence of larger aerosol concentration. Examining aerosol–cloud-meteorology interplay is not the focus of this work; however, the contrasting seasonality in observed f_c over the Arabian Sea and Bay of Bengal, and the South Indian Ocean signifies the importance of understanding the climatology of cloud vertical structure in this region. This is required to improve our understanding of aerosol–cloud interaction in all seasons in these regions, since the relative vertical distributions of aerosols and clouds influence aerosol–cloud interaction (Chand et al. 2009).

3.2. *Climatology of cloud vertical distribution*

MISR-derived mean monthly $\boldsymbol{f_c}$ from surface to 20 km altitude at 0.5 km altitude bins is shown in the top panel of Figure 4. Dominance of low-level clouds in the first 3 km over all the three ocean basins is noticeable throughout the year. Mid-to-high-level clouds are observed to evolve over the Arabian Sea and Bay of Bengal during the monsoon season. On the contrary, the South Indian Ocean shows no seasonality in mid-to-high-level clouds; instead, there is an increment in the low clouds during the monsoon season (June–September). Mean ($\pm 1\sigma$) annual f_c of low clouds (summing f_c up to 3.5 km altitude) over the Arabian Sea, Bay of Bengal, and South Indian Ocean are 0.34 ± 0.06,

0.24 ± 0.05, and 0.39 ± 0.11, respectively. Corresponding values for the mid-level (sum of f_c between 3.5 and 6.5 km) and high clouds (sum of f_c above 6.5 km) are 0.08 ± 0.02, 0.08 ± 0.01, and 0.16 ± 0.15 and 0.19 ± 0.07, 0.32 ± 0.07, and 0.21 ± 0.10, respectively. Annually, low clouds contribute 57%, 34%, and 55% to f_c (in relative terms with respect to columnar f_c as reported in Table 1) over the Arabian Sea, Bay of Bengal, and South Indian Ocean, respectively, while the corresponding relative contributions of high clouds are 31%, 46%, and 30%, respectively.

Since ground truth data do not exist in this case to evaluate the MISR statistics, the vertical structure of clouds is examined using GOCCP data (bottom panel of Figure 4). The active sensor can detect multilayer clouds within the same pixel and hence can be considered as more accurate than a passive sensor. Our analysis reveals a large amount ($f_c > 0.3$) of high-level clouds at ~14–16 km over the Arabian Sea and Bay of Bengal, especially during the monsoon season. More uniform monthly f_c at this altitude range is observed over the South Indian Ocean relative to the other two regions. In the tropics, large f_c at such high altitudes may be attributed to the anvil cirrus (Folkins, Oltmans, and

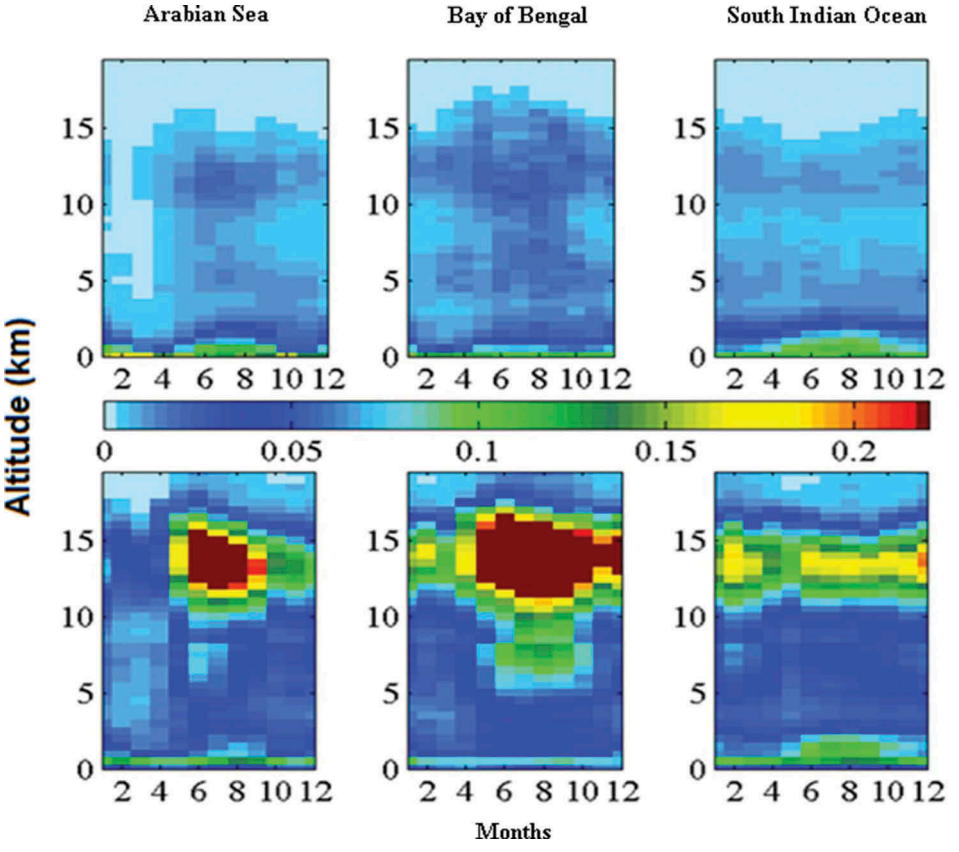

Figure 4. Mean monthly climatology of f_c at 0.5 km altitude bins from the surface to 20 km altitude using MISR data for the period March 2000–February 2010 (top panel) and at 0.8 km altitude bins from the surface to 19.2 km using GOCCP data for the period June 2006–February 2010 (bottom panel) over the Arabian Sea, Bay of Bengal, and South Indian Ocean. Months (in X-axis) are represented by numbers starting from 1 (January) to 12 (December).

Thompson 2000), which was confirmed by GOCCP SR profiles. MISR fails to detect cirrus clouds whose optical depth is below 0.3 (Prasad and Davies 2012), while the GOCCP detects clouds with COD > 0.07 (Chepfer et al. 2010). Instead, MISR can see through thin cirrus clouds and detect low clouds by the stereo technique. We note that GOCCP values theoretically represent frequency occurrence of clouds at each altitude bin, which should be kept in mind while carrying out direct comparison between absolute values of f_c from MISR and GOCCP. During the monsoon season, there is an overall increase in f_c over the Arabian Sea and Bay of Bengal. The increase in f_c with height, especially over the Arabian Sea and Bay of Bengal where cloud heights reach 10–15 km, is an indication of the formation of deep convective clouds over these basins. The high-intensity winds transport moisture northwards from the South Indian Ocean leading to large convective activity over the Arabian Sea and Bay of Bengal resulting in the formation of convective clouds (Mohanty et al. 2002). However, such seasonal change in cloud vertical structure is not observed over the South Indian Ocean. Monthly variations of f_c of low-level clouds are similar for MISR and GOCCP. Slightly high bias in MISR statistics relative to GOCCP may be attributed to the 'clear conservative' cloud mask approach of MISR (Zhao and Di Girolamo 2006), which detects any pixel as completely cloudy even if it is partially filled by clouds. Hence, this approach overestimates f_c in the tropical regions dominated by small cumulus clouds (e.g. Jones, Di Girolamo, and Zhao 2012). Low bias in low-level cloudiness in GOCCP data may also result from the masking effect of high clouds, as noted by Konsta, Chepfer, and Dufresne (2012). Climatology of cloud vertical structure from MISR for the same period as of GOCCP does not change the overall conclusion.

To gain further understanding of the multilayer cloud field over the oceans as seen from GOCCP and MISR statistics, the ISCCP D2 data set is also analysed to derive mean monthly contributions of each individual cloud type to f_c (Figure 5). Climatologically, differences in mean annual f_c of low, mid-level, and high clouds from ISCCP and MISR are −9%, 3%, and 8%, respectively, over the Arabian Sea. Over the Bay of Bengal, ISCCP- and MISR-retrieved f_c of low clouds are similar, while ISSCP overestimates mid-level cloud by 9% and underestimates high clouds by 5% relative to MISR. ISCCP underestimates the f_c of low, mid-level, and high

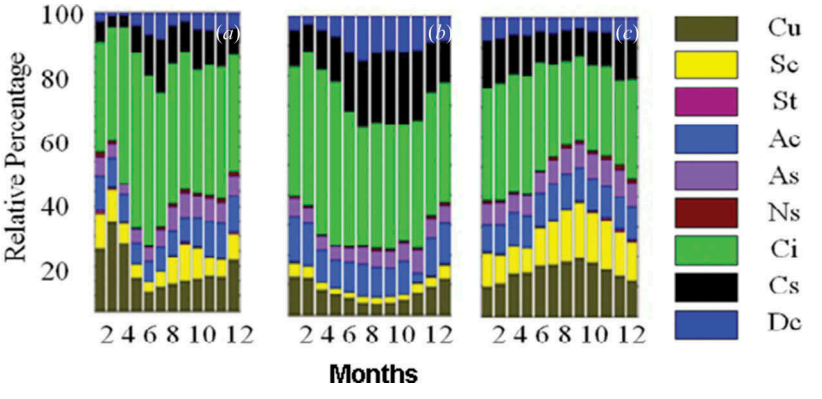

Figure 5. Monthly statistics of relative abundance of the individual cloud types from ISCCP over the (*a*) Arabian Sea, (*b*) Bay of Bengal, and (*c*) South Indian Ocean for the period January 2000–December 2007. Months (in *X*-axis) are represented by numbers starting from 1 (January) to 12 (December). 'Cu', 'Sc', 'St', 'Ac', 'As', 'Ns', 'Ci', 'Cs', and 'Dc' represent 'cumulus', 'stratocumulus', 'stratus', 'altocumulus', 'altostratus', 'nimbostratus', 'cirrus', 'cirrostratus', and 'deep convective' clouds, respectively.

clouds by 7%, 3%, and 5%, respectively, relative to MISR over the South Indian Ocean. On the other hand, high clouds are found to occur more frequently (similar to GOCCP) than other cloud types, with the mean annual values of 65% over the Bay of Bengal, 61% over the Arabian Sea, and 51% over the South Indian Ocean (Figure 5). Cirrus dominates among the high clouds throughout the year (as also shown by Meenu et al. (2010)). However, the relative abundance of deep convective clouds shows a strong seasonal cycle consistent with the monsoon circulation in this region. Cumulus and altocumulus dominate among the low- and mid-level clouds, respectively, and their relative abundances are higher during the post-monsoon and winter seasons over the Arabian Sea and Bay of Bengal compared to other seasons (Bony, Collins, and Fillmore 2000). Reduction in relative abundances of cumulus and stratocumulus clouds in the ISCCP data during the monsoon season may be attributed to evolution of deep convective clouds. Over the South Indian Ocean, the high clouds in ISCCP data do not show much variation seasonally (Figure 5(*c*)), consistent with the GOCCP data, while the increment in low clouds (as observed in both MISR and GOCCP data in Figure 4) during June–September is attributed to increase in cumulus and stratocumulus clouds (Figure 5(*c*)).

Overall, the cloud climatology derived from ISCCP complements the MISR-derived climatology. Since cloud is detected by a radiometric technique in the ISCCP data set, low-level clouds are difficult to identify if there is an appreciable amount of high-level clouds such as cirrus in the same pixel. MISR, on the other hand, uses the calibration-insensitive stereo technique, and thus can detect low clouds beneath thin cirrus. Thus by combining passive sensors MISR and ISCCP, a multilayer cloud field can be interpreted as seen in the GOCCP data set (active sensor) in this region (Marchand et al. 2010). However, we note that the cloud detection thresholds are different in these data sets. For example, sub-visual cirrus may still cause a bias in quantitative comparison between ISCCP-MISR combined climatology and GOCCP climatology.

The cloud distributions in day and night-time over these regions are also examined using the GOCCP data. The mean seasonal differences in f_c vertical structure over the Arabian Sea, Bay of Bengal, and South Indian Ocean are shown in Figure 6. The diurnal variation in day and night-time f_c vertical distribution is largest (with f_c larger in daytime by >20%) in the monsoon season below 8 km over all the three regions. The diurnal

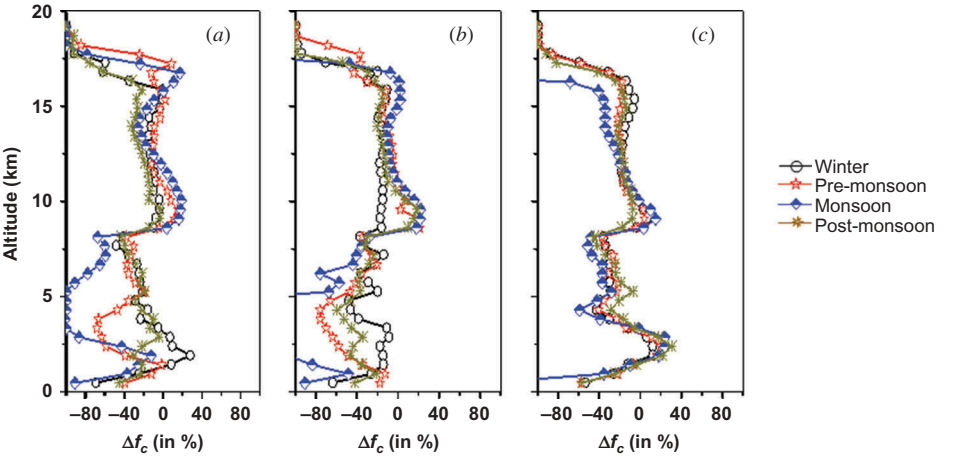

Figure 6. Variation of Δf_c (difference in night-time f_c with respect to daytime f_c, in %) with altitude for four seasons over the (*a*) Arabian Sea, (*b*) Bay of Bengal, and (*c*) South Indian Ocean.

variation is almost similar in all the seasons over the Arabian Sea and Bay of Bengal (Figures 6(*a*) and (*b*)), while it is larger in the monsoon relative to other seasons over the South Indian Ocean above 8 km (Figure 6(*c*)). Larger f_c of low clouds is observed in night-time relative to daytime over the Arabian Sea during the winter season and over the South Indian Ocean (between 1 and 3 km altitudes) during all the seasons. The seasonality in diurnal difference of cloud vertical structure is overall weaker over the South Indian Ocean than the other two ocean basins. Throughout the year, night-time f_c from passive sensor (MODIS) is observed to be slightly larger relative to the statistics from the active (GOCCP) sensor over the three ocean basins (Table 1).

4. Discussion and Conclusions

In this article, we have presented the climatology of cloud vertical structure over the oceanic regions adjacent to the Indian subcontinent using multi-year passive and active remote-sensing data. Such multi-sensor comparison helps in understanding the realistic 3-D distribution of clouds in view of the strengths and limitations of the sensors and their different retrieval techniques, as advocated by Stubenrauch et al. (2013**)**. The vertical distribution of clouds shows strong seasonal variability that may have several implications for the regional climate. Previously, during the Indian Ocean Experiment (Ramanathan, Crutzen, Lelieveld, et al. 2001) and afterwards (e.g. Chylek et al. 2006), strong evidence of aerosol indirect and semi-direct effect over the North Indian Ocean was reported. A more recent study (Dey et al. 2011) found evidence of a transition from aerosol indirect to semi-direct effect on shallow cumulus clouds in this region. The possible influence of changes in cumulus cloud cover in response to aerosol forcing on the formation of deep convection needs to be examined in future. Moreover, the large amount of low clouds (along with larger aerosol loading) in our climatology over the Arabian Sea and Bay of Bengal relative to the South Indian Ocean during the post-monsoon and winter seasons may result in a latitudinal asymmetry in SST due to radiative feedback. Whether this interpretation holds true, and if yes, whether that influences the monsoon circulation, requires detailed investigation. Many researchers (e.g. Ramanatahn et al. 1989; Rajeevan and Srinivasan 1999) have shown that the net CRF (i.e. balance between SW cooling and LW warming) depends on the cloud vertical distribution. Therefore, the statistics presented here may help in better interpretation of the seasonal variation of net CRF (an important component of the climate forcing) in this region. These results will further help in understanding the climate model performances in simulating clouds in this region, which is critical to quantify the cloud radiative feedback (Soden and Vecchi 2011). For example, large overestimation of high clouds by the CAM4 model is observed over the Bay of Bengal (Zhang et al. 2012). However, for such a comparison, it should be noted that satellite data are not ground truth; and in fact, considerable discrepancy may exist in observed vertical structure (although columnar f_c may be similar) as reported here. The multi-sensor statistics presented here will be useful for this purpose.

The major conclusions of the present study are as follows.

(1) f_c shows strong seasonal variability over the Arabian Sea and Bay of Bengal with the highest values (>0.7) during June–July and the lowest values (0.3–0.4) during February–March. It remains greater than 0.6 throughout the year over the South Indian Ocean without much seasonal variability as shown by both passive and active sensors. This may be attributed to lack of development of convective

clouds during June–September as opposed to other seasons, as observed in the Arabian Sea and Bay of Bengal.

(2) The true cloud vertical structure is better resolved by active sensors (such as GOCCP). MISR detects low clouds beneath thin cirrus using the stereo technique, but underestimates cirrus clouds with respect to GOCCP. ISCCP detects thin cirrus using a radiometric technique, but fails to detect low clouds beneath them. Thus, a combination of passive remote-sensing data from MISR and ISCCP qualitatively complements the cloud vertical structure as seen by GOCCP in this region.

(3) Low clouds (mostly cumulus and stratocumulus) increase, while cirrus decreases over the South Indian Ocean during the northern hemispheric summer monsoon season. On the other hand, the relative contribution of high clouds (mostly cirrostratus and deep convective clouds) increases over the Arabian Sea and Bay of Bengal (larger increase over the Bay of Bengal relative to the Arabian Sea) during the monsoon season. Annually, cumulus, altocumulus, and cirrus dominate the low, mid-level, and high clouds, respectively, in all the three regions with strong seasonal cycle.

(4) Diurnal variation (day vs. night comparison) in f_c vertical structure is similar in all four seasons over the South Indian Ocean, while it is larger in the monsoon season over the Arabian Sea and Bay of Bengal. During the monsoon, f_c during daytime below 8 km altitude is larger (by >40%) than that in night-time over these regions.

(5) The multi-sensor statistics presented here suggest that climate model performances in simulating cloud vertical structure in this region should not be evaluated against one particular passive sensor. Even for an active sensor, there may be a low bias in 'low cloud' if optically thick clouds exist aloft.

Acknowledgements

We acknowledge the comments from two anonymous reviewers that helped in improving the earlier version of the manuscript.

Funding

This research is supported by the Ministry of Earth Sciences, Government of India under the CTCZ programme (MoES/CTCZ/16/28/10) through a research grant operational at IIT Delhi (IITD/IRD/RP02479). MISR, MODIS, ISCCP and CERES data are obtained from the NASA Langley Research Center and GOCCP data are obtained from LMD/IPSL (http://climserv.ipsl.polytechnique.fr/cfmip-obs/Calipso_goccp.html).

References

Ackerman, S., K. Strabala, P. Menzel, R. Frey, C. Moeller, L. Gumley, B. Baum, S. W. Seeman, and H. Zhang. 2002. *Discriminating Clear-Sky from Cloud with MODIS Algorithm Theoretical Basis Documents (MOD35), MODIS Documentation*. http://modis.gsfc.nasa.gov/data/atbd/atbd_mod06.pdf

Altaratz, O., I. Koren, L. A. Remer, and E. Hirsch. 2014. "Review: Cloud Invigoration by Aerosols -Coupling between Microphysics and Dynamics." *Atmospheric Research* 140–141: 38–60. doi:10.1016/j.atmosres.2014.01.009.

Anselmo, T., R. Cliton, W. Hunt, K.-P. Lee, T. Murray, K. Powell, S. D. Rodier, M. Vaughan, O. Chomette, M. Viollier, O. Hagolle, A. Lifermann, A. Garnier, J. Pelon, J. C. Currey, M Pitts,

and D. Winker. 2007. *Cloud-Aerosol LIDAR Infrared Pathfinder Satellite Observations (CALIPSO) Data Products Catalog*. http://csyotc.cira.colostate.edu/documentation/CALIOP/CALIPSO_DPC_Rev2x4.pdf

Bony, S., W. D. Collins, and D. Fillmore. 2000. "Indian Ocean Low Clouds during the Winter Monsoon." *Journal of Climate* 13: 2028–2043. doi:10.1175/1520-0442(2000)013<2028:IOLCDT>2.0.CO;2.

Chand, D., R. Wood, T. L. Anderson, S. K. Satheesh, and R. J. Charlson. 2009. "Satellite-Derived Direct Radiative Effect of Aerosols Dependent on Cloud Cover." *Nature Geoscience* 2: 181–184. doi:10.1038/ngeo437.

Chepfer, H., S. Bony, D. Winker, G. Cesana, J. L. Dufresne, P. Minnis, C. J. Stubenrauch, and S. Zeng. 2010. "The GCM Oriented CALIPSO Cloud Product (CALIPSO-GOCCP)." *Journal of Geophysical Research* 115: D00H16. doi:10.1029/2009JD012251.

Chylek, P., M. K. Dubey, U. Lohmann, V. Ramanathan, Y. J. Kaufman, G. Lesins, J. Hudson, G. Altmann, and S. Olsen. 2006. "Aerosol Indirect Effect over the Indian Ocean." *Geophysical Research Letters* 33: L06806. doi:10.1029/2005GL025397.

Dash, S. K., M. A. Kulkarni, U. C. Mohanty, and K. Prasad. 2009. "Changes in the Characteristics of Rain Events in India." *Journal of Geophysical Research* 114 (D10): D10109. doi:10.1029/2008JD010572.

Dey, S., and L. Di Girolamo. 2010. "A Climatology of Aerosol Optical and Microphysical Properties over the Indian Subcontinent from 9 Years (2000-2008) of Multiangle Imaging Spectroradiometer (MISR) Data." *Journal of Geophysical Research* 115: D15204. doi:10.1029/2009JD013395.

Dey, S., L. Di Girolamo, G. Zhao, A. L. Jones, and G. M. McFarquhar. 2011. "Satellite-Observed Relationships between Aerosol and Trade-Wind Cumulus Cloud Properties over the Indian Ocean." *Geophysical Research Letters* 38: L01804. doi:10.1029/2010GL045588.

Di Girolamo, L., A. Menzies, G. Zhao, K. Mueller, C. Moroney, and D. J. Diner. 2010. "Level 3 Cloud Fraction by Altitude Algorithm Theoretical Basis." JPL D–62358. http://eospso.gsfc.nasa.gov/sites/default/files/atbd/MISR_CFBA_ATBD.pdf

Eastman, R., S. G. Warren, and C. J. Hahn. 2011. "Variations in Cloud Cover and Cloud Types over the Ocean from Surface Observations, 1954-2008." *Journal of Climate* 24: 5914–5934. doi:10.1175/2011JCLI3972.1.

Folkins, I., S. Oltmans, and A. Thompson. 2000. "Tropical Convective Outflow and near Surface Equivalent Potential Temperatures." *Geophysical Research Letters* 27: 2549–2552. doi:10.1029/2000GL011524.

Gadgil, S., P. V. Joseph, and N. V. Joshi. 1984. "Ocean-Atmosphere Coupling over Monsoon Regions." *Nature* 312: 141–143. doi:10.1038/312141a0.

Goren, T., and D. Rosenfeld. 2014. "Decomposing Aerosol Cloud Radiative Effects into Cloud Cover, Liquid Water Path and Twomey Components in Marine Stratocumulus." *Atmospheric Research* 138: 378–393. doi:10.1016/j.atmosres.2013.12.008.

Goswami, B. N., V. Venugopal, D. Sengupta, M. S. Madhusoodan, and P. K. Xavier. 2006. "Increasing Trend of Extreme Rain Events over India in a Warming Environment." *Science* 314 (5804): 1442–1445. doi:10.1126/science.1132027.

IPCC (Intergovernmental Panel on Climate Change). 2007. Climate Change 2007: The physical basis: contribution of working group I to the Fourth Assessment Report, Chapter 2.

Jin, X., J. Hanesiak, and D. Barber. 2007. "Detecting Cloud Vertical Structures from Radiosondes and MODIS over Arctic First-Year Sea Ice." *Atmospheric Research* 83: 64–76. doi:10.1016/j.atmosres.2006.03.003.

Jones, A. L., L. Di Girolamo, and G. Zhao. 2012. "Reducing the Resolution Bias in Cloud Fraction from Satellite Derived Clear-Conservative Cloud Masks." *Journal of Geophysical Research* 117: D12201. doi:10.1029/2011JD017195.

Kedia, S., S. Ramachandran, T. A. Rajesh, and R. Srivastava. 2012. "Aerosol Absorption over Bay of Bengal during Winter: Variability and Sources." *Atmospheric Environment* 54: 738–745. doi:10.1016/j.atmosenv.2011.12.047.

Klein, S. A., Y. Zhang, M. D. Zelinka, R. Pincus, J. Boyle, and P. J. Gleckler. 2013. "Are Climate Model Simulations of Clouds Improving? An Evaluation Using the ISCCP Simulator." *Journal of Geophysical Research* 118 (3): 1329–1342. doi:10.1002/jgrd.50141

Konsta, D., H. Chepfer, and J.-L. Dufresne. 2012. "A Process Oriented Characterization of Tropical Oceanic Clouds for Climate Model Evaluation, Based on A Statistical Analysis of Daytime A-

Train Observations." *Climate Dynamics* 39 (9–10): 2091–2108. doi:10.1007/s00382-012-1533-7.

Kühnlein, M., T. Appelhans, B. Thies, A. A. Kokhanovsky, and T. Nauss. 2013. "An Evaluation of a Semi-Analytical Cloud Property Retrieval Using MSG SEVIRI, MODIS and Cloudsat." *Atmospheric Research* 122: 111–135. doi:10.1016/j.atmosres.2012.10.029.

Loeb, N., and G. L. Schuster. 2008. "An Observational Study of the Relationship between Cloud, Aerosol and Meteorology in Broken Low-Level Cloud Conditions." *Journal of Geophysical Research* 113: D14214. doi:10.1029/2007JD009763.

Maddux, B. C., S. A. Ackerman, and S. Platnick. 2010. "Viewing Geometry Dependencies in MODIS Cloud Products." *Journal of Atmospheric and Oceanic Technology* 27: 1519–1528. doi:10.1175/2010JTECHA1432.1.

Marchand, R., T. Ackerman, M. Smyth, and W. B. Rossow. 2010. "A Review of Cloud Top Height and Optical Depth Histograms from MISR,ISCCP, and MODIS." *Journal of Geophysical Research* 115. doi:10.1029/2009JD013422.

Marchand, R. T., T. P. Ackerman, and C. Moroney. 2007. "An Assessment of Multiangle Imaging Spectroradiometer (MISR) Stereo-Derived Cloud Top Heights and **C**loud Top Winds Using Ground-Based Radar, Lidar and Microwave Radiometers." *Journal of Geophysical Research* 112: D06204. doi:10.2029/2006JD009191.

Meenu, S., K. Rajeev, and K. Paramaeswaran. 2011. "Regional and Vertical Distribution of Semitransparent Cirrus Clouds over the Tropical Indian Region Derived from CALIPSO Data." *Journal of Atmospheric and Solar-Terrestrial Physics* 73: 1967–1979.

Meenu, S., K. Rajeev, K. Parameswaran, and A. K. M. Nair. 2010. "Regional Distribution of Deep Clouds and Cloud Top Altitudes over the Indian Subcontinent and the Surrounding Oceans." *Journal of Geophysical Research* 115: D5. doi:10.1029/2009JD11802.

Mohanty, U. C., R. Bhatla, P. V. S. Raju, O. P. Madan, and A. Sarkar. 2002. "Meteorological Fields Variability over the Indian Seas in Pre and Summer Monsoon Months during Extreme Monsoon Seasons." *Earth and Planetary Science* 111 (3): 365–378.

Nair, A. K. M., K. Rajeev, S. Sijikumar, and S. Meenu. 2011. "Characteristics of a Persistent 'Pool of Inhibited Cloudiness' and Its Genesis over the Bay of Bengal Associated with the Asian Summer Monsoon." *Annals of Geophysics* 29: 1247–1252. doi:10.5194/angeo-29-1247-2011.

Naud, C., J. P. Muller, M. Haeffelin, Y. Morille, and A. Delaval. 2004. "Assessment of MISR and MODIS Cloud Top Heights through Inter-Comparison with a Back-Scattering Lidar at SIRTA." *Geophysical Research Letters* 31 (4): L04114. doi:10.1029/2003GL018976.

Patil, S. D., and R. K. Yadav. 2005. "Large-Scale Changes in the Cloud Radiative Forcing over the Indian Region." *Atmospheric Environment* 39 (26): 4609–4618. doi:10.1016/j.atmosenv.2005.03.051.

Platnick, S., M. D. King, S. A. Ackerman, W. P. Menzel, B. A. Baum, J. C. Riedi, and R. A. Frey. 2003. "The MODIS Cloud Products: Algorithms and Examples from Terra." *IEEE Transactions on Geoscience and Remote Sensing* 41 (2): 459–473.

Prasad, A. A., and R. Davies. 2012. "Detecting Tropical Thin Cirrus Using Multiangle Imaging Spectroradiometer's Oblique Cameras and Modeled Outgoing Longwave Radiation." *Journal of Geophysical Research* 117 (D6): D06208.

Probst, P., R. Rizzi, E. Tosi, V. Lucarini, and T. Maestri. 2012. "Total Cloud Cover from Satellite Observations and Climate Models." *Atmospheric Research* 107: 161–170.

Rajeevan, M., and J. Srinivasan. 1999. "Net Cloud Radiative Forcing at the Top of Atmosphere in the Asian Monsoon Region." *Journal of Climate* 13: 650–657.

Ramanathan, V., R. D. Cess, E. F. Harrison, P. Minnis, B. R. Barkstrom, E. Ahmad, and D. Hartmann. 1989. "Cloud Radiative Forcing and Climate: Results from the Earth Radiation Budget Experiment." *Science* 243: 57–63.

Ramanathan, V., P. J. Crutzen, J. T. Kiehl, and D. Rosenfeld. 2001. "Aerosols, Climate and the Hydrological Cycle." *Science* 294: 2119–2124.

Ramanathan, V., P. J. Crutzen, J. Lelieveld, A. P. Mitra, D. Althausen, J. Anderson, M. O. Andreae, W. Cantrell, G. R. Cass, C. E. Chung, A. D. Clarke, J. A. Coakley, W. D. Collins, W. C. Conant, F. Dulac, J. Heintzenberg, A. J. Heymsfield, B. Holben, S. Howell, J. Hudson, A. Jayaraman, J. T. Kiehl, T. N. Krishnamurti, D. Lubin, G. McFarquhar, T. Novakov, J. A. Ogren, I. A. Podgorny, K. Prather, K. Priestley, J. M. Prospero, P. K. Quinn, K. Rajeev, P. Rasch, S. Rupert, R. Sadourny, S. K. Satheesh, G. E. Shaw, P. Sheridan, and F. P. J. Valero. 2001.

"Indian Ocean Experiment: An Integrated Analysis of the Climate Forcing and Effects of the Great Indo-Asian Haze." *Journal of Geophysical Research* 106. doi:10.1029/2001JD900133.

Ramanathan, V., M. V. Ramana, G. Roberts, D. Kim, C. E. Corrigan, C. E. Chung, and D. Winker. 2007. "Warming Trends in Asia Amplified by Brown Cloud Solar Absorption." *Nature* 448: 575–578.

Randall, D., S. Krueger, C. Bretherton, J. Curry, P. Duynkerke, M. Moncrieff, B. Ryan, D. Starr, M. Miller, W. Rossow, G. Tselioudis, and B. Wielick. 2003. "Confronting Models with Data, the GEWEX Cloud Systems Study." *Bulletin of the American Meteorological Society* 84: 455–469.

Rossow, W. B., and R. A. Schiffer. 1999. "Advances in Understanding Clouds from ISCCP." *Bulletin of the American Meteorological Society* 80: 2261–2288.

Sathiyamoorthy, V., P. K. Pal, and P. C. Joshi. 2011. "Influence of the Upper-Tropospheric Wind Shear upon Cloud Radiative Forcing in the Asian Monsoon Region." *Journal of Climate* 17 (14): 2725–2735.

Smirnov, A., B. N. Holben, I. Slutsker, D. M. Giles, C. R. McClain, T. F. Eck, S. M. Sakerin, A. Macke, P. Croot, G. Zibordi, P. K. Quinn, J. Sciare, S. Kinne, M. Harvey, T. J. Smyth, S. Piketh, T. Zielinski, A. Proshutinsky, J. I. Goes, N. B. Nelson, P. Larouche, V. F. Radionov, P. Goloub, K. Krishna Moorthy, R. Matarrese, E. J. Robertson, and F. Jourdin. 2009. "Maritime Aerosol Network as a Component of Aerosol Robotic Network." *Journal of Geophysical Research* 114: D06204.

Soden, B. J., and G. A. Vecchi. 2011. "The Vertical Distribution of Cloud Feedback in Coupled Ocean-Atmosphere Models." *Geophysical Research Letters* 38: L12704. doi:10.1029/2011GL047632.

Stubenrauch, C. J., W. B. Rossow, S. Kinne, S. Ackerman, G. Cesana, H. Chepfer, L. Di Girolamo, B. Getzewich, A. Guignard, A. Heidinger, B. C. Maddux, W. P. Menzel, P. Minnis, C. Pearl, S. Platnick, C. Poulsen, J. Riedi, S. Sun-Mack, A. Walther, D. Winker, S. Zeng, and G. Zhao. 2013. "Assessment of Global Cloud Datasets from Satellites: Project and Database Initiated by the GEWEX Radiation Panel." *Bulletin of the American Meteorological Society* 94: 1031–1049.

Verlinden, K. L., D. W. J. Thompson, and G. L. Stephens. 2011. "The Three-Dimensional Distribution of Clouds over the Southern Hemisphere High Latitudes." *Journal of Climate* 24: 5799–5811.

Wonsick, M. M., R. T. Pinker, and Y. Govaerts. 2009. "Cloud Variability over the Indian Monsoon as Observed from Satellites." *Journal of Applied Meteorology and Climatology* 48: 1803–1821.

Wu, D. L., S. A. Ackerman, R. Davies, D. J. Diner, M. J. Garay, B. H. Kahn, B. C. Maddux, C. M. Moroney, G. L. Stephens, J. P. Veefkind, and M. A. Vaughan. 2009. "Vertical Distributions and Relationships of Cloud Occurrence Frequency as Observed by MISR, AIRS, MODIS, OMI, CALIPSO and Cloudsat." *Geophysical Research Letters* 36: L09821. doi:10.1029/2009GL037464.

Wylie, D. P., W. P. Menzel, and K. I. Strabala. 1994. "Four Years of Global Cirrus Cloud Statistics Using HIRS." *Journal of Climate* 7: 1972–1986.

Xi, B., X. Dong, P. Minnis, and M. M. Khaiyer. 2010. "A 10 Year Climatology of Cloud Fraction and Vertical Distribution Derived from Both Surface and GOES Observations over the DOE ARM SPG Site." *Journal of Geophysical Research* 115: D12124. doi:10.1029/2009JD012800.

Zhang M. H., W. Y. Lin, S. A. Klein, J. T. Bacmeister, S. Bony, R. T. Cederwall, A. D. Del Genio, J. J. Hack, N. G. Loeb, U. Lohmann, P. Minnis, I. Musat, R. Pincus, P. Stier, M. J. Suarez, M. J. Webb, J. B. Wu, S. C. Xie, M.-S. Yao, and J. H. Zhang. 2005. "Comparing Cloud and Their Seasonal Variation in Ten Atmospheric General Circulation Models with Satellite Measurements." *Journal of Geophysical Research* 110: D15S02. doi:10.1029/2004JD005021.

Zhang, Y., S. Xie, C. Covey, D. D. Lucas, P. Gleckler, S. A. Klein, J. Tannahill, C. Doutriaux, and R. Klein. 2012. "Regional Assessment of the Parameter-Dependent Performance of CAM4 in Simulating Tropical Clouds." *Geophysical Research Letters* 39: L14708.

Zhao, G., and L. Di Girolamo. 2006. "Cloud Fraction Errors for Trade Wind Cumuli from EOS-Terra Instruments." *Geophysical Research Letters* 33: L20802. doi:10.1029/2006GL027088.